Upscaling of regional models into basin-wide models

Vandenbulcke Luc[1,2] and Barth Alexander[3]

[1]seamod.ro, Jailoo srl, Romania
[2]MAST, Université de Liège, Belgium
[3]GHER, Université de Liège, Belgium

Correspondence: Luc Vandenbulcke (luc@seamod.ro)

Abstract. Traditionnally, in order for lower-resolution, global- or basin-scale models to benefit from some of the improvements available in higher-resolution regional or coastal models, two-way nesting has to be used. This implies that the parent and child models have to be run together and there is an online exchange of information between both models. This approach is often impossible in operational systems, where different model codes are run by different institutions, often in different countries. Therefore, in practice, these systems use one-way nesting with data transfer only from the large-scale model to the regional models. In this article, it is examined whether it is possible to replace the missing feedback (coming from the child model) by data assimilation, avoiding the need to run the models simultaneously. Selected variables from the high-resolution forecasts will be used as pseudo-observations, and assimilated in the lower-resolution models. The method will be called "upscaling".
A realistic test-case is set up with a model covering the Mediterranean Sea, and a nested model covering its North-Western basin. Under the hypothesis that the nested model is, in some sense, more realisic than the parent model, the upscaling method is implemented. Two simulations of the parent model are then compared: the case of one-way nesting (or stand-alone model), and a simulation using the upscaling technique on the temperature and salinity variables. It is shown that the representation of some processes, such as the Rhône river plume, are strongly improved in the upscaled model compared to the stand-alone model.

1   Introduction

In the present-day operational oceanography landscape, services are provided at different scales by different expert centers. At the European Union level, the Copernicus Marine Environment Monitoring Service (CMEMS) provides reanalyses, analyses and forecasts at global and basin scales. The models for the different basins are run by different institutes and centers within the regional monitoring and forecasting centers. Various regional and coastal oceanographic centers then use the CMEMS products to provide initial and/or boundary conditions to their respective models. These regional and coastal models benefit from the increased experience and specific knowledge of the local teams in their particular area of interest. Furthermore, local models usually run at higher resolution, and may include more accurate data (bathymetry, river discharge data...) and processes of smaller scales, that cannot be easily included into basin-scale models. High resolution observations such as satellite sea surface temperature (SST), and recent ultra-high resolution products (see e.g. Le Traon et al., 2015) have been shown to be best assimilated into nested models, as chances are higher that the observed processes are well represented (Vandenbulcke et

al, 2006). Similarly, high-resolution current observations by high-frequency radars are expected to benefit most to models with a similar high resolution (i.e. nested models).

When large-scale and regional or coastal models are run together (meaning, concurrently and on the same computing platform), it is possible to use two-way nesting; the benefits mentioned above of using a regional or coastal model are then transferred back to the basin-scale model. This has been shown numerous times in the literature, e.g. Barth et al. (2005); Debreu et al. (2012). The beneficial impact of the feedback from regional-scale to the basin-scale forecasts is visible even outside the domain of the regional model. This constitutes the baseline hypothesis of the present study: it is desirable to "copy" the results of the nested model into the parent model.

To emulate this nesting feedback, missing in the operational context, it is analyzed whether forecasts from the regional model can be used as pseudo-observations and assimilated in the basin-scale model. Indeed, data assimilation is not limited to the use of (real) observations by measurement devices. Onken et al. (2005) used data assimilation as a substitute for one-way nesting in a cascade of nested models. Alvarez et al. (2000) used a statistical model to predict SST, which was then assimilated as pseudo-observations in a hydrodynamic model (Barth et al., 2006). In the proposed "upscaling" method, the pseudo-observations come from the nested model. From the point of view of the forecasting centers, a data assimilation scheme is already implemented in the basin-scale model. Hence, implementing the upscaling method requires only to obtain the high-resolution forecasts and assimilate them (along with the real observations) during the analysis phase of the system.

When using grid nesting, problems at the open boundary of the child model include stratification mismatches, artificial waves, artificial rim currents; and ultimately instabilities and model blow-up (Mason et al., 2010; Debreu et al., 2012). By upscaling the child model into the parent model, the latter will progressively gain consistency with the child model solution within its domain, being beneficial for the child model over time. Upscaling can potentially reduce the risk of discrepancies at the open sea boundary.

Upscaling can also be seen as using a regional or coastal model as a "measurement device" that replaces ever-too-sparse (real) measurements. Guinehut et al. (2002, 2004) showed that a coverage of the North Atlantic with a $3°$-resolution grid of Argo floats allows to effectively represent the large scales. Using a $5°$ array reduces the precision of the estimated fields two times. Currently, some CMEMS areas are largely undersampled.

Upscaling can be understood as a complement to downscaling (initialization) techniques such as presented in Auclair et al. (2000, 2001) (VIFOP) or in Simoncelli et al. (2011). The point of these methods is to combine interpolated fields coming from the large-scale model (the background or first-guess field) and existing high-resolution fields, so that small-scale structures present in coastal models are not lost whenever it is (re)-initialized by fields interpolated from the basin-scale model, and the obtained fields are physically balanced with respect to the coastal physics. If upscaling is used to improve the basin-scale fields

and accord them with the coastal model, the "first guess" will be already much better.

Schulz-Stellenfleth and Stanev (2016) is another recent example showing the benefits of two-way nesting, especially in sophisticated modern-day forecasting systems. The study demonstrates that two-way nesting is critical for correct energy transfers between large and small scales (especially in coupled ocean-wave-atmosphere models) for cross-border advection, for the correct use of high-resolution coastal observations that cannot be fed directly into a large-scale model, etc. Ackowledging that operational systems are using only one-way nesting, Schulz-Stellenfleth and Stanev (2016) therefore strongly advocate the research into "upscaling" techniques. The present article tries to develop precisely such a technique.

In this article, the upscaling procedure is tried out in a realistic, nested model configuration covering the Mediterranean Sea and the North-Western basin and simulating the year 2014. The same model, NEMO 3.6 (Madec, 2008), and the same vertical resolution, are used for both configurations (only the horizontal grid is different). This could influence the conclusion compared to a set-up with 2 different model codes. However, this is not expected to be a fundamental limitation of the method. Concerning the vertical grid, in the usual case of assimilating real observations such as vertical profiles, the observations and model forecasts have different vertical resolutions. Similarly, if the child model were on a different vertical grid than the parent model, it would still contain useful information, worth to be assimilated in the parent model. A limitation could be that some of the observations may be lost, e.g. the lowest child model layer may be out-of-grid in the parent model.

If different model codes were used, the modes could represent different processes. Hence, this should be taken into account by modifying the (representativity part of the) observation error covariance matrix when performing the data assimilation of the pseudo-observations. Examples of such contributions to the representativity error could be

- different vertical coordinates (see above)

- different implementations of the ocean surface: rigid lid or free surface; for the latter, linear or non-linear representation

- hydrostatic model or not

- different atmospheric forcing fields

- different turbulent closure schemes

- different numerical schemes for advection, horizontal diffusion etc.

The most striking difference between the parent and child models however, remains the horizontal resolution, and therefore, the general conclusions of the paper are expected to be valid, and upscaling should not be limited to the case of parent and child models being identical.

In this study, it is not the aim to verify that the nested model is indeed more realistic, according to some metrics, than the parent model. Rather, this consistutes the baseline hypothesis, and thus it is always considered beneficial to bring the parent

model forecast closer to the child model forecast. It should be noted that some high-resolution processes, resolved by the nested model but not by the parent model, could have large phase errors in the nested model. In this case, the baseline hypothesis would be violated, and the nested model could actually have higher errors than the former. This aspect is not considered in the paper.

5   The models and data assimilation scheme are described in section 2. Section 3 proposes some metrics to evaluate the system, related to the Rhône river plume, the cross-shelf exchanges, the large-scale current, SST, and the formation of Western Mediterranean Deep Water. Results are given in section 4 and a conclusion in presented in section 5.

2   Model and data assimilation configuration

10 ### 2.1   Hydrodynamic model

The upscaling technique has been implemented in the North-Western Mediterranean Sea, including the Gulf of Lions and the Ligurian Sea. The latter is characterized by large-scale currents (the Northern Current also called Liguro-Provencal Current, created by the junction of the Eastern and Western Corsican Currents, see e.g. Pinardi et al. (2015)), by intense meso-scale activity and by inertial oscillations. Furthermore, the NW-Med is the siege of formation of Western Mediterranean Deep Water

15 (WMDW), important to the circulation in the whole Mediterranean Sea (e.g. Millot, 1999; Pinardi et al., 2015; Bosse et al., 2015; Somot et al., 2018; Simoncelli and Pinardi, 2018).

A realistic, one-way nested configuration was implemented using the NEMO 3.6 model and the AGRIF nesting tool (Debreu et al., 2008), covering respectively the Mediterranean Sea (MED) with a 6 km horizontal resolution, and the North-Western

20 Mediterranean basin (NW-Med). The parent model resolution is similar to the previous version of the CMEMS Mediterranean Sea analysis-forecasting system (up to October 2017) and to the present reanalysis (1/16°). The bathymetry of the nested model (1/80°) is more realistic than the parent model, at the coastline and more importantly, at the different canyons at the Gulf of Lions shelf break. Supplementary details of the model configuration are given in the Appendix (A1).

When implementing the upscaling method, it is expected that after some time, the feedback from the NW-Med model will mod-

25 ify the Northern Current position and intensity in the MED model, which will in turn influence the NW-Med model through its open-sea boundary. The boundary condition provided by the MED model also influences the stratification of the water column, which is important for the pre-conditionning of the convection (S. Somot, private communication).

Both model bathymetries are interpolated from the GEBCO bathymetry. The temperature and salinity initial condition is inter-

30 polated from the CMEMS Mediterranean reanalysis (1/16°) for 01/01/2014 (see https://doi.org/10.25423/medsea_reanalysis_ phys_006_004). The model starts from rest. Atmospheric fluxes are computed using bulk formula; the atmospheric forcing fields are obtained from ECMWF ERA Interim with a temporal resolution of 3 hours and a horizontal resolution of 0.75° reinterpolated by the ECMWF server to 0.125° (Dee et al., 2011). In the MED model, the flow between the Black Sea and

the Mediterranean Sea, through the Marmara Sea and the Dardanelles Strait, is modelized as a river, using climatological flow, temperature and salinity values. The salinity of the incoming water has a minimum and maximum of 22.5 psu and 27.5 psu reached in July and March respectively. Five other rivers (Rhône, Po, Ebro, Nile, Drin) are also represented, and monthly climatologic values for the flow and temperature are used, whereas the salinity is put to 5 psu, except for the Drin river where is it put at 2 psu. Using climatologic monthly values is coherent with the operational set-up in the CMEMS Mediterranean system, although the latter represents many more small rivers.

Daily Rhone river discharge measurements at the Beaucaire station were obtained from the Compagnie du Rhône, in order to be used in the nested NW-Med model. Interestingly, the total annual flow computed from the climatology and from the measured values for 2014-2015 are very similar (1% difference). However seasonal and daily values can be very different (see Fig. 1a). In particular, during the considered period, the climatology underestimates the winter discharge, but overestimates the summer discharge. Hence, depending on the dataset used, it is expected that the modelled river plume will also be significantly different. This is illustrated in Fig 1b, showing the difference in surface salinity obtained with the nested model at the end of January 2014. The plume obtained using real river discharge extends much further offshore, almost completely across the Gulf of Lions, whereas the plume obtained with the climatological river discharge is essentially staying at the coast close to the river mouth. This is consistent with the much larger (almost double) discharge values observed in the real river data during January 2014.

2.2 Upscaling experiment description, Ensemble generation, and Data Assimilation scheme

In order to assimile pseudo-observations into the basin-scale models, different setups could be implemented, regarding the choice of the pseudo-observations, the frequency of assimilation, the data assimilation scheme itself, etc. The choices described below are consistent with current-day practices in the CMEMS operational systems. In particular, none of them currently assimilates velocity fields, and all of them use parameterized model state vector error covariances. Only one system (the Arctic system) currently uses an Ensemble Kalman filter, but the other systems are planning to evolve toward ensemble simulations in the future. The following settings were chosen for the current experiment. The filter is an Ensemble Kalman filter, some details are given in the annex. Assimilation will be performed daily. Only temperature and salinity will be used as pseudo-observations but the whole (thinned) 3D fields will be used. Velocity and surface elevation are not updated by the data assimilation procedure. Thinning is realized by taking the average of 5x5 cells of the nested model. The thinned pseudo-observations coming from the nested model are then considered independent, i.e. their error covariance matrix is diagonal. This is still a strong assumption which should be taken into account when determining the (diagonal) part of the observation error covariance matrix. The members of the ensemble have perturbed initial conditions, atmospheric forcing fields and Rhône river discharge, similar to Auclair et al. (2003).

The initial condition is the randomly weighted sum of the real initial condition (01/01/2014), and 6 other initial conditions (1 year, 20 days and 10 days earlier, and 10 days, 20 days and 1 year later). The weight of the real initial condition is a random-normal number chosen in the Gaussian distribution with mean 0.5 and standard deviation 0.2; if necessary, the random number is then limited back into [0.2 0.8], whereas the 6 remaining weights are random numbers chosen uniformly in [0 1],
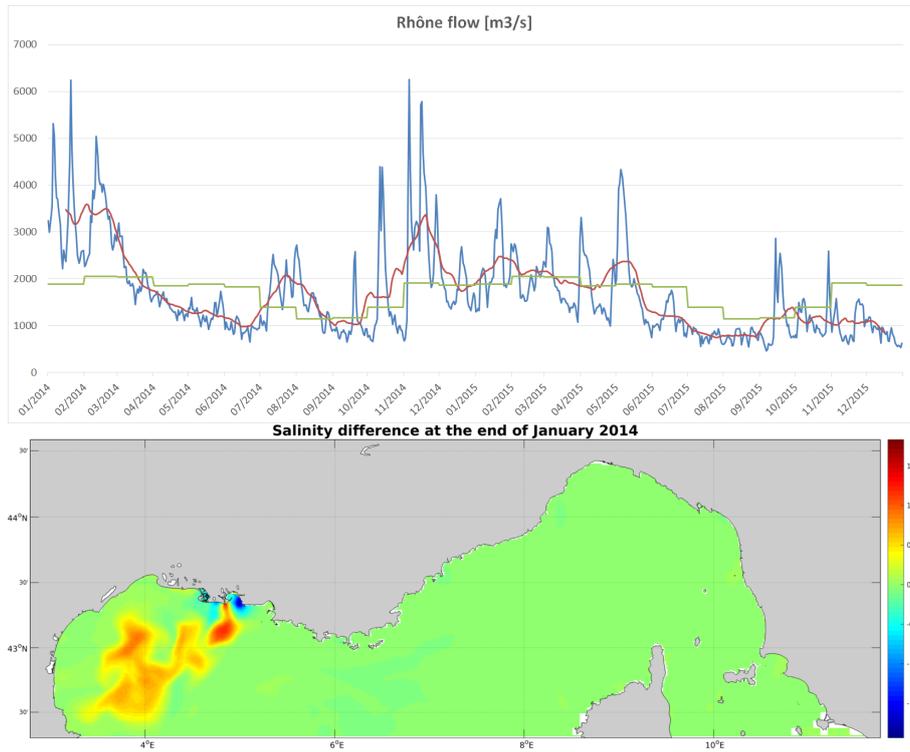
Figure 1. (above) Rhône river discharge from (green) the climatology, (blue) the measurements by the Compagnie du Rhone at the Beaucaire station, (red) the 1-month moving average of the measurements. (below) Difference of surface salinity in 2 different model runs of the nested grid on 28/Jan/2014, when using climatological or measured Rhône discharge values (i.e. using the green or blue curve in the upper panel)

.

and normalized so that the sum of all 7 weights is 1. This procedure ensures that the stability of each member is not modified (for example, the linear combination of 7 stable water columns is still a stable water column).

The atmospheric forcing fields of air temperature at 2m height and wind speed at 10m height are perturbed following the same procedure as in Barth et al. (2011); Vandenbulcke et al. (2017). Point-wise, the forcing fields are decomposed in Fourier series (from 3 hours to 1 year). For each member, a random field is generated, using these Fourier modes and random coefficients which have a temporal correlation length corresponding to the respective mode. This random field is added to the original field. The Rhône river discharge is perturbed using a random walk approach, with the expected perturbation after one year set as 20%. The other rivers are outside the observed part of the domain, and their discharge is not perturbed. With all 3 perturbations, an ensemble of 100 members is then spun up for 1 month.

Data assimilation is performed by the Ocean Assimilation Kit (OAK) package (Barth et al., 2008) implementing different filters such as SEEK and the Ensemble Kalman filter (EnKF). Different variants of the EnKF exist, and are classified in

stochastic and deterministic methods. The former require to perturb the observations, adding sampling noise. The latter, also called Ensemble Square Root Filters, do not present this requirement; the perturbation approach is only applied in the model to obtain model errors. Different variants are compared in Tippett et al. (2003). One variant, called the Ensemble Transform Kalman Filter (Bishop et al., 2001; Wang et al., 2004), is used in this study. The filter equations are listed in Barth and Vandenbulcke (2017).

Nerger et al. (2012) summarizes how the spurious long-range correlations can be suppressed using so-called covariance localization, or domain localization and its addition observation localization. OAK uses the latter variant introduced in Hunt et al. (2007). In essence, the state vector is split into subdomains (water columns). In every water column, the analysis is performed independently (domain localization). In addition, for every water column, only nearby observations are used and the inverse of their error variance is multiplied by a localization function (observation localization). In the current setup, the localization function is a radial Gaussian function with an e-folding distance of 30 km.

The observation errors for temperature and salinity are set respectively at 0.3°C and 0.09 psu. These values were determined after a sensitivity experiment with observation errors of (0.5°C, 0.15 psu), (0.3°, 0.09 psu), (0.2°C, 0.05 psu) or (0.1°C, 0.03 psu); as a trade-off between generating a close emulation of two-way nesting (hence very small observation errors), and generating fields as balanced as possible, that will not cause adjustment shocks into the model (hence larger observation errors). With the latter 2 choices for the observation error, the obtained assimilation increment was not much larger than with the final choice of (0.3°, 0.09 psu), but qualitatively, unrealistic small scale variations started to appear.

From a technical point of view, OAK allows to use a multi-variate multi-grid state vector. As the Mediterranean model is paralized in 64 tiles, the multi-grid feature allows to update directly the tiles from the Mediterranean model restart files, influenced by the nested model, without including the other tiles in the state vector. The procedure thus allows to skip the reconstruction of the complete Mediterranean restart files. It should be noted that the tiles of the parent model, considered in the data assimilation procedure, are the ones covering the nested-model area, but also the neighbouring ones which are influenced by the data assimilation.

3 Metrics

To assess the upscaling method, five metrics were defined, that allow to compare the nested model to both the basin-scaled model without upscaling (free model) and with upscaling. If upscaling is succesfull, the basin-scale model with upscaling will be closer to the nested model, than its counterpart without upscaling.

3.1 Cross-shelf transport

The penetration of off-shore water on the GoL (or inversely when negative transport values are obtained), is critical for the circulation on the shelf, for the shelf-open sea exchanges, etc. It is obtained by integrating the current over the boundary shown in Fig. 2. This metric is useful to compare basin-scale models (free and upscaled) and check whether the upscaling procedure
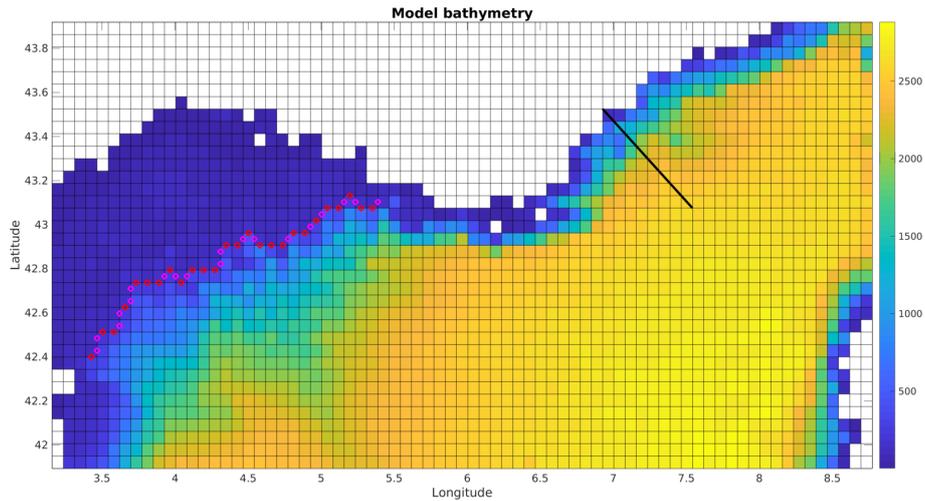
Figure 2. Zoom of the MED model grid, with the positions for computing the Northern Current metric (black line) and the cross-shelf transport metric (magenta and red dots)

is able to drive the solution toward the nested model solution. The intensity of the cross-shelf transport cannot, however, be compared to real measurements (by lack of them).

3.2 Northern Current intensity

The Northern Current (NC) is the most important large-scale feature of the region of interest. It is considered to have a width
5 of 40-50km during summer and 20-30km during winter; but the most offshore currents do not modify the transport much. Similarly, the NC is considered to be 100-200m deep in summer and 250-400m in winter. Following Alberola et al. (1995), its intensity is obtained by integrating the currents normal to a line from Nice to the location (43.0756°N, 7.5415°E), 214 km to the South-East, indicated in Fig. 2. As for the previous one, this metric only allows to inter-compare different models.

3.3 Rhône river plume

10 The plume of the Rhône River is measured by selecting all points around the river mouth with a salinity smaller than 37psu, and then choosing the most distant one from the river mouth. This provides the plume length and direction, although it may be an approximation: the plume can be curved, in which case its real length is larger than the estimation, or it can cover a large area, in which case the algorithm still obtains an azimuth although in reality it is not well defined.
This metric can be used quantitatively to compare models. Furthermore, it can be used to compare model results to real mea-
15 surements. Indeed, although the real Rhône river plume length and direction are not measured directly, they can be estimated from satellite chlorophyll-a images. The model-observations comparison is then qualitative.

3.4 Sea surface temperature

This metric is the root mean square (rms) difference between the model and observed SST. For the latter, the L3 images are used. Furthermore, in order to examine the position of features such as fronts and eddies, the rms difference of the norm of the spatial gradient of the SST is also computed.

3.5 Western Mediterranean Deep Water formation

Following Bosse et al. (2015) and references herein, the formation zone of Western Mediterranean Deep Water (WMDW) is comprised in 41-43°N, 4-6°E. WMDW forms an easily identifiable area in the temperature-salinity diagram, and the present-day characteristics are: temperature of 12.86~12.89°C, salinity of 38.48~38.50 psu, depth is larger than 1000 m. The nested model (NW-Med) southern boundary is at 42.3°N, and hence only a part of the formation zone is included in the area of MED covered by pseudo-observations. Furthermore, the WMDW tail in the modeled temperature-salinity diagram is longer, with the following characteristics: temperature of 12.7~12.89°C and salinity of 38.4~38.5 psu. The metric measures the total volume [m^3] of WMDW in the domain covered by the NW-Med model, and is used to compare the different models.

4 Results

The temperature difference between the (unperturbed) parent and child models at the end of the spinup (31 January 2014) is represented in Fig. 3 on the child model grid. There are large temperature differences at the shelf break of the Gulf of Lions (the canyons are much better represented in the regional model); which extend all the way from the surface to the bottom of the Gulf of Lions. Other large differences appear in the Eastern and Western Corsican Currents, and their junction resulting in the Northern Current, as well as at the southern open boundary. The difference in salinity (not shown) has large values around the Rhône river plume (over 1 psu), and in a lesser extent in the Eastern Corsican Current. It appears that after a month, the differences are already significant, and if one trusts the regional model more, then it would be beneficial to bring these differences back to the basin-scale model.

At the end of the spin-up, the spread of the ensemble of models (Fig. 4) is very visible over the basin, at all river mouths, but also in other regions (Alboran Sea, Tunesian coastal zone...) as all 3 perturbations are applied at once. The ensemble spread is also visible in depth (i.e. deeper than when only the river discharge is modified).

As an example, the first data assimilation cycle is shown in Fig. 5 depicting SST. Qualitatively, it appears that upscaling changes important features: the Rhône river plume is oriented offshore instead of being mostly along-shore; fronts seem to be more well-defined; and the Northern Current flows along the shelf break instead of covering a large part of the shelf. The nested model, and the "upscaled" model, seem to be in closer agreement with the satellite image, than the free model.
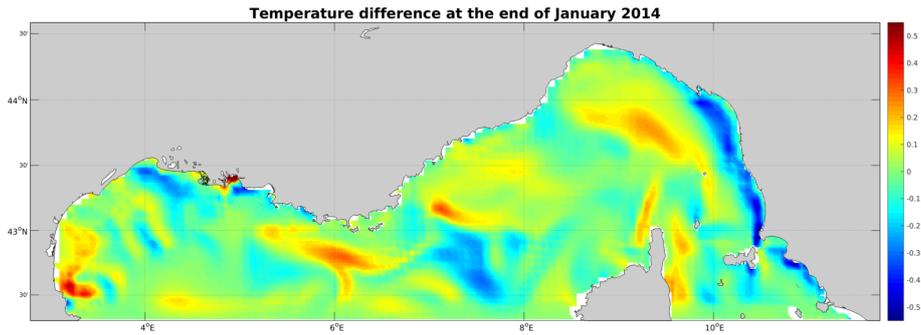
Figure 3. Temperature difference between the parent and nested models at 31/01/2014, projected on the nested model grid.
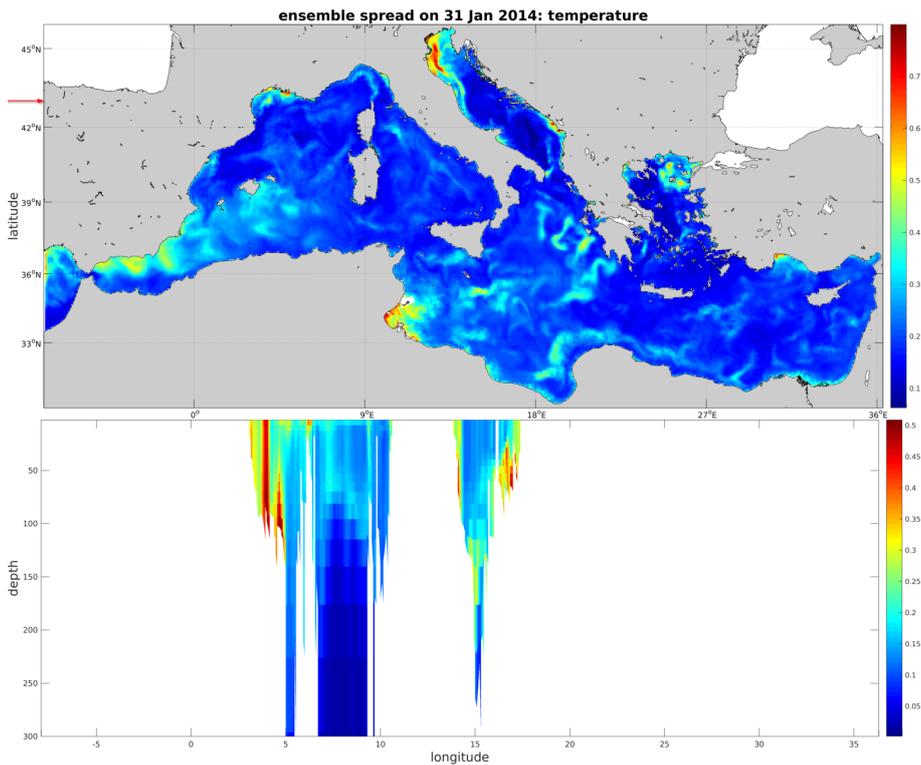
Figure 4. Spread of the ensemble of MED models at 31/01/2014: (upper panel) surface temperature, (lower panel) section at 43°N, indicated by a red arrow on the upper panel

4.1 Cross-shelf transport

The flow accross the shelf break is represented in Fig. 6, for the basin-scale model in the free and upscaled cases. Although alternating periods of inflow and outflow appear, the transport seems to show a chaotic behavior. Yet it can be seen that while both models are generally similar, some periods exist where the simulated transport is very different. During the first month
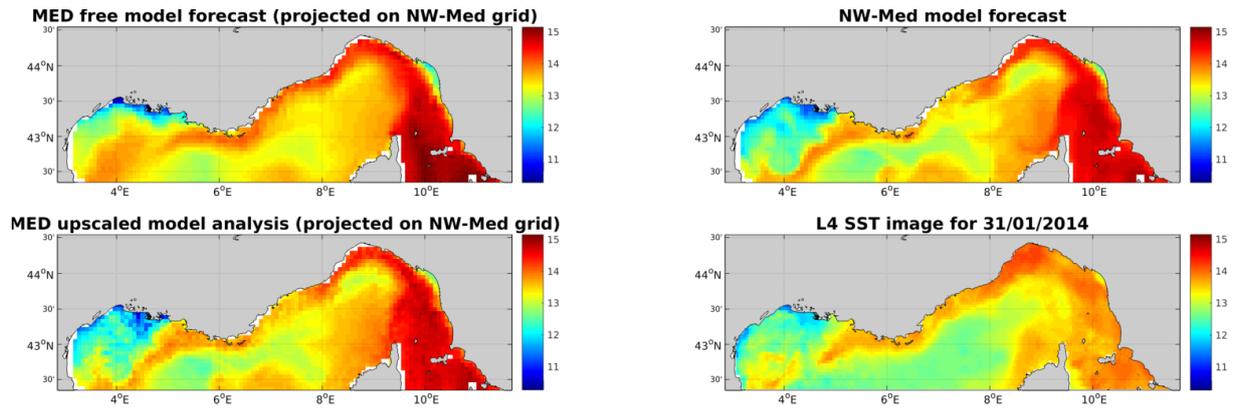
Figure 5. Sea surface temperature after the first upscaling step (31/01/2014), in the free model (upper left), nested model (upper right), upscaled model (lower left) and satellite observation (lower right)

(February 2014), the free model predicts a net outflow during the first 2 weeks, followed by a net inflow during the last 2 weeks. The nested model (not shown) and hence also the upscaled model actually predicts the exact opposite. The reasons for the nested model to behave differently than the parent model may be an effect of wind interaction with the (different) bathymetries, or related to the different resolution. The actual transport is not measured or available; but the result of interest

5 here is that the upscaling method is able to align the (parent model) currents with the ones from the nested model, and hence emulate two-way nesting, although only temperature and salinity pseudo-observations are used.

During the remainder of the year, the upscaled model predicts somewhat larger transports (both inward and outward). Generally speaking however, the two transport curves are closer than in February (or at least they are not of opposite signs anymore). Noticeably, in August-September, the upscaled model predicts a period of large inflow on the Gulf of Lions. The free model

10 also predicts this inflow, but delayed by about 2 weeks.

4.2 Northern Current

The transport by the Northern Current off Nice is represented in Fig. 7. Over the whole period, the root mean square difference between parent and nested models is 0.22 Sv for the free model, and 0.19 Sv for the upscaled model. The same qualitative observations can be made as for the cross-shelf transport. Both models generally agree, but periods exist with relatively impor-

15 tant differences. Interestingly, a large difference appears in August-September, when the free model predicts a larger transport than the upscaled model. This is also the period when the transport accross the shelf break presents a temporal shift in between models.

For the purpose of our study, this metric cannot be used to validate the model since real measurements of the Northern Current transport are not available; but (as for the previous metric), it can be used to compare models, and to show that our goal is

20 reached and upscaling of scalar fields is able to modify the velocity field of the parent model although only temperature and salinity are observed.
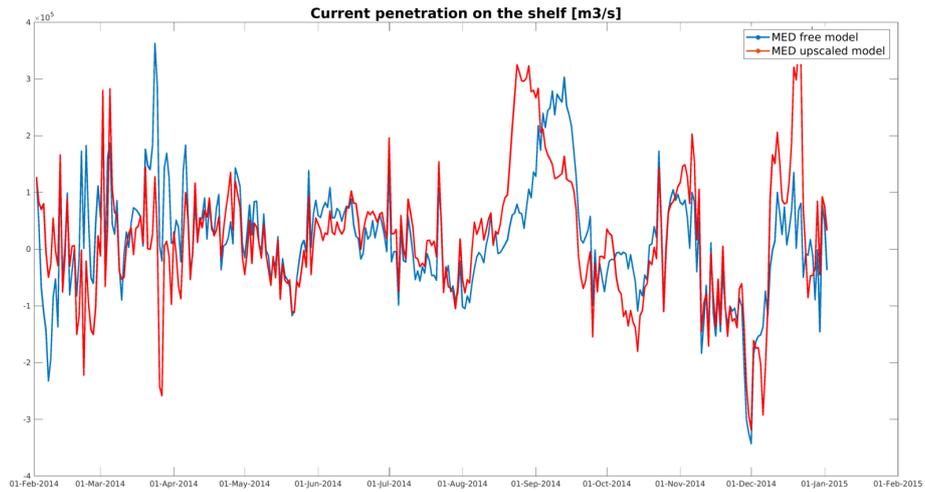
Figure 6. Water transport accross the shelf break during 2014, as obtained by the free (blue curve) and upscaled (red curve) parent models. Positive values indicate a net on-shelf transport.
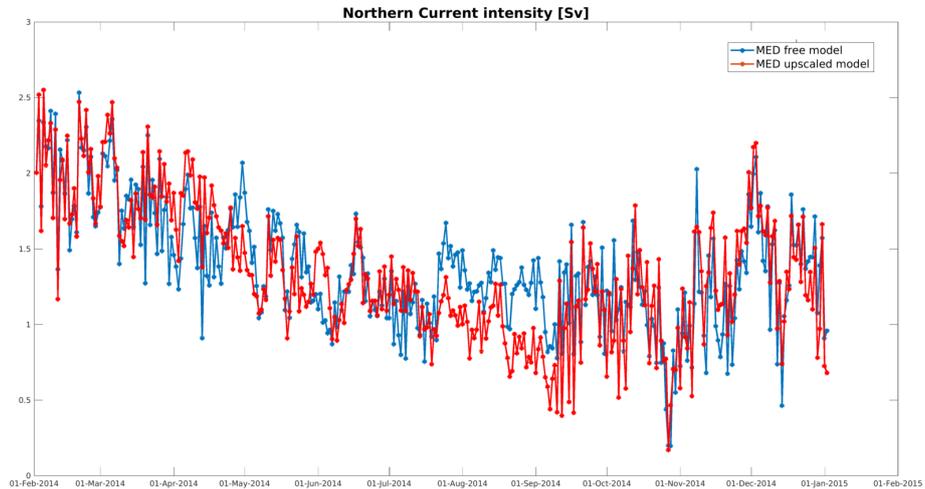
Figure 7. Water transport by the Northern current off Nice (France) during 2014, as obtained by the free (blue curve) and upscaled (red curve) parent models.

4.3 River plume

The Rhône plume metric is perhaps the metric most significantly altered by upscaling. During the first month of the upscaled simulation, the free model usually places the plume along-shore, to the North-East, whereas the nested model usually orients the plume off-shore to the South-East (see Fig. 8). On top of the resolution-related differences between parent and nested models (in particular the bathymetry and the interaction of the water masses with the wind), both models have different freshwater
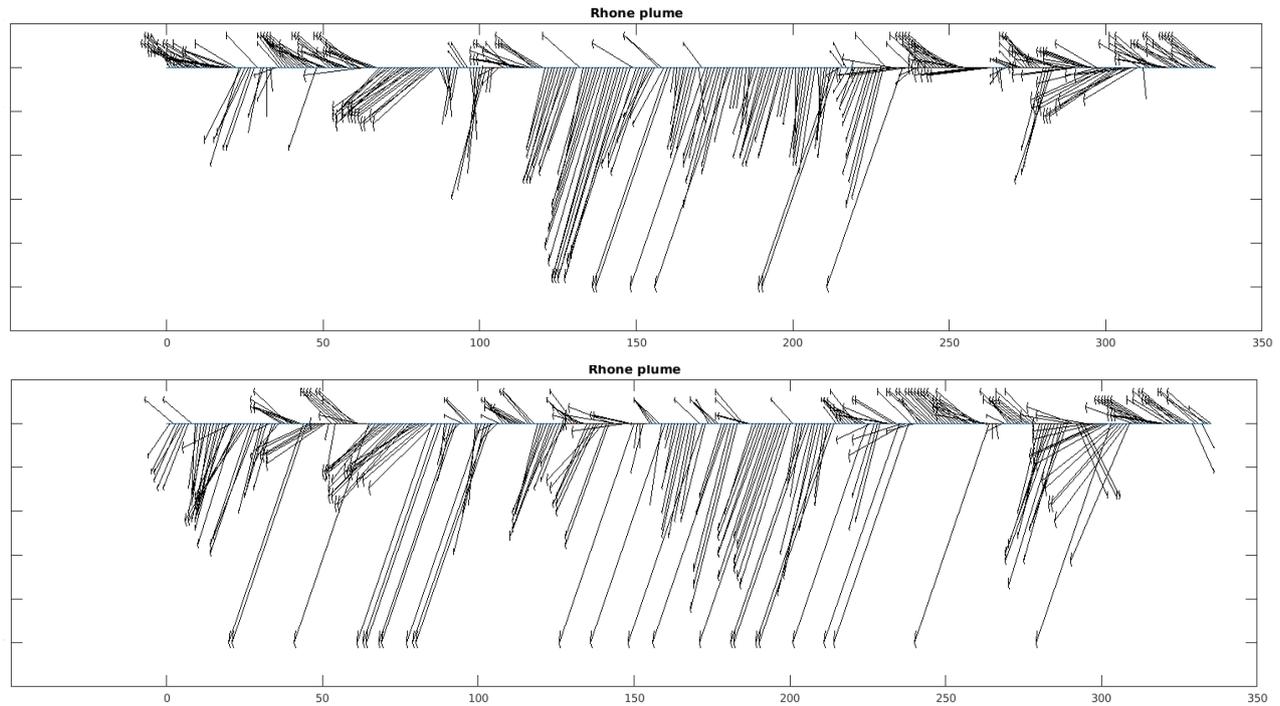
Figure 8. Rhône river plume direction and length (upper panel) for the free and (lower panel) upscaled MED models. The horizontal scale represents the days after the start of the upscaling experiment (Feb/2014).

discharge values, which is usually much higher and has also a much larger variability in the nested model during February 2014. The upscaling method is clearly able to make the parent model ingest the different plume dynamic coming from the nested model. During the remainder of 2014, differences between both models are smaller, with another period (late August - early September) where the opposite case occurs: the free model plume is oriented off-shore, but the nested (and upscaled) model predicts an along-shore plume.

The river plume can qualitatively be compared to real observations by using satellite observations of chlorophyll. During the first month of simulation, where the most significant differences appear, only a few level-3 satellite images are not almost entirely obscured by clouds. An example is given in Fig. 9 for 12 February 2014. One can clearly see the off-shore plume from the chlorophyll observations, whereas the free model plume is mostly along-shore. The nested and upscaled models correctly place the plume off-shore. Apart from the surface salinity used to characterize the Rhône plume, upscaling also modifies in-depth salinity. In particular, the cores of the Eastern and Western Corsican Currents are saltier in the upscaled model, with differences of about 0.15 psu during the first assimilation cycle.
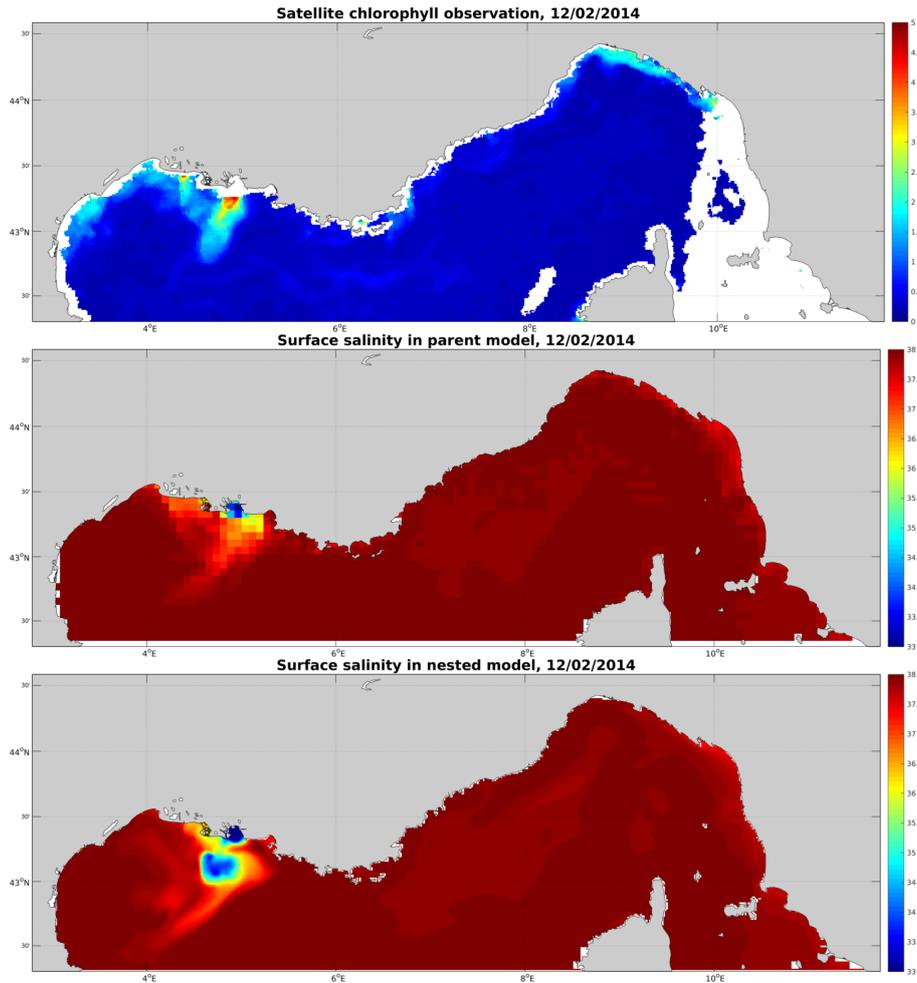
Figure 9. Comparison of the Rhône river plume on 12/Feb/2014 (upper panel) satellite chlorophyll image (middle panel) free parent model salinity (lower panel) and nested model salinity

4.4 SST

The sea surface temperature metric allows to quantify the model error by comparison with satellite images. Level 3 images are used for computing the metric (a level 4 image shown in Fig. 5 is used only for visual comparison). Results are shown in Fig. 10. It appears that generally, the (parent) model is already in very good agreement with observations, even though no data assimilation is performed. Usually, the nested model is better still in some areas (e.g. coastal waters), and the upscaling procedure brings back these local improvements to the parent model. However, the area-wide RMS error is not influenced very much by upscaling, as large areas are essentially unmodified (parent and child models use the same atmospheric forcing fields). Some days, some processes appear to be missed by the models (both parent and nested), so that the RMS error is relatively large. In this case again, upscaling does not influence the RMS error of the parent model very much, as the nested model is not
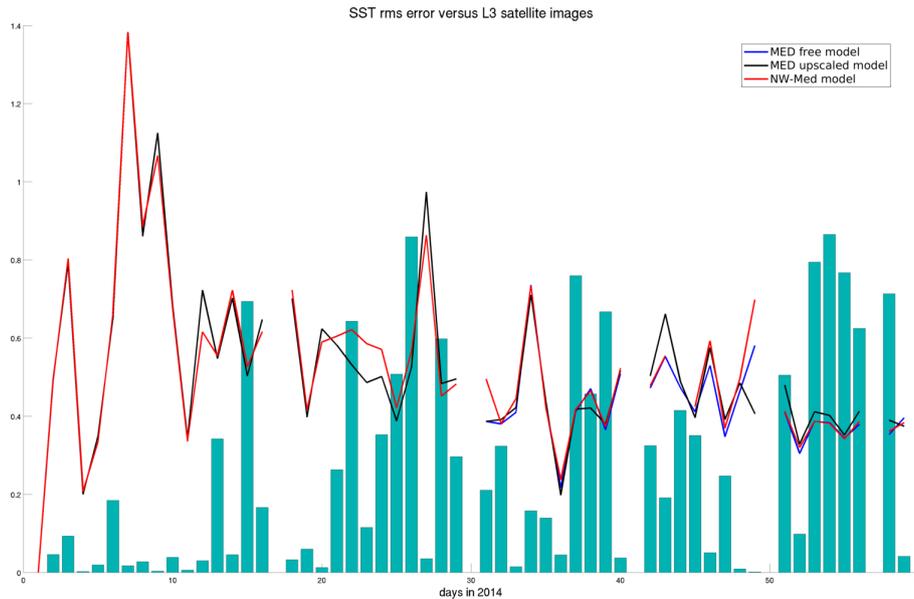
Figure 10. SST RMS error in the free model (black curve), nested model (red curve), upscaled model (blue curve) during the first 2 months of simulation. The bars represent the proportion of unclouded points in the L3 satellite image.

representing these processes any better than the parent model.

In both cases, this does not imply that the upscaling method is flawed, but rather that, in the current setup, the nested model is not able to generate an RMS error significantly lower than the parent model; hence upscaling does not have much to feed on. Fig. 10 shows the RMS error during the first 2 months of simulation. A similar plot for the whole of 2014 shows that the

5 situation worsens during summer (errors of 3°C) both for parent and child model; the difference in between models is hidden by the temporal variability of the error (not shown). In any case, the upscaled model is still very close, and slightly better, than both the (free) parent and the nested models.

The model temperature in depth can be only punctually evaluated against observations (when e.g. drifter observations are available). In any case, the goal of the current study is to check whether upscaling is able to bring the parent model closer to

10 the nested model, under the hypothesis that the latter is "better" in some sense. Differences between the parent and the nested model are locally important, e.g. on the bottom of the Gulf of Lions, or in the Eastern Corsican and Northern Current cores (with differences of up to 0.3°C), and upscaling is able to push the temperature field in the parent model toward the nested model solution.

4.5 WMDW

15 The total amount of Western Mediterranean Deep Water in the free model (blue curve in Fig. 11) and the nested model (green curve) is periodically important (10^3km^3), and both models do not appear to converge during the simulation. On the contrary, a period of large discrepency appears during most of the second half of the year. Upscaling largely modifies the parent model,
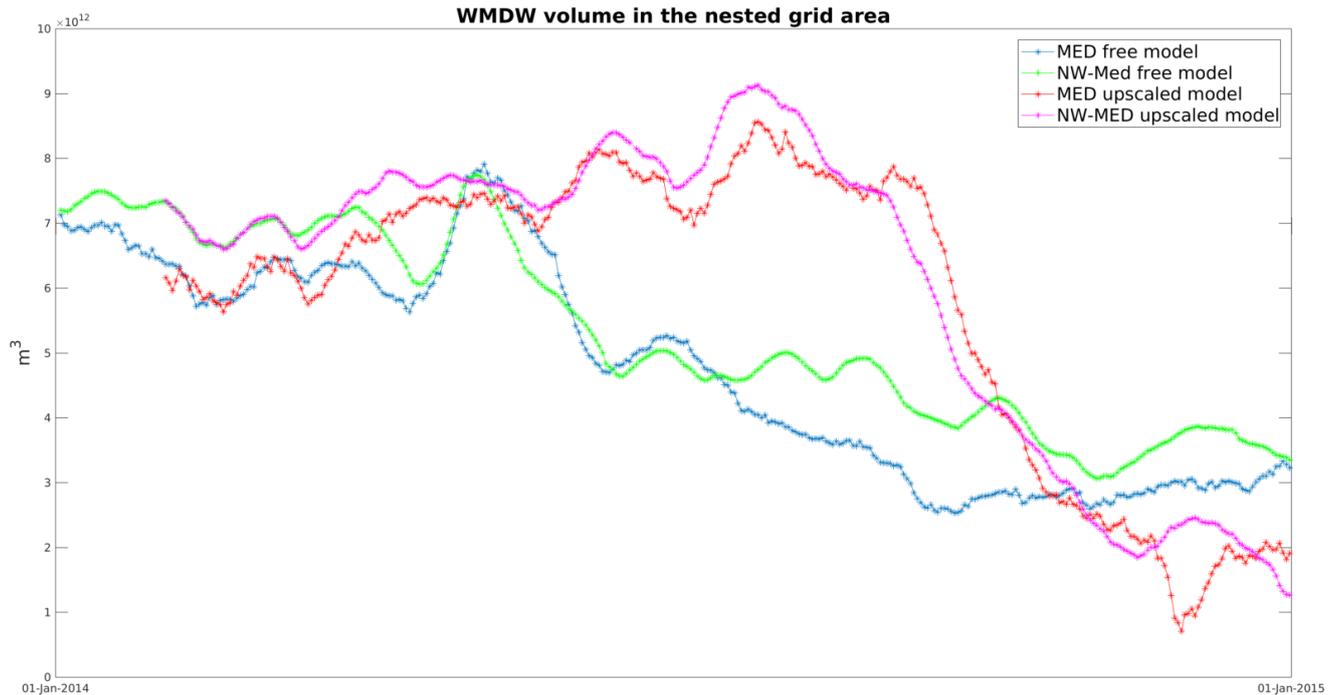
Figure 11. Time serie of total amount of WMDW in the area covered by the nested model: (blue) free parent model (green) nested model in the free model (red) parent model with upscaling (magenta) nested model in the upscaled model

which in turns provides modified boundary conditions to the nested model, so that after a while, the upscaled model and its child model significantly diverge from the free models. Without measurements and due to the choice of the model domain, it is not possible to assert which pair of models is more realistic. However, as for other metrics, the discrepency between parent and child model is reduced in the upscaled pair of models, which is certainly a desirable characteristic. This can be explained by the fact that the data assimilation also modifies the parent model solution outside the nested area (in the limit of the localization radius used in the data assimilation procedure). Therefore, the water immediately outside the nested domain is modified and made more coherent with the nested solution. East and West of Corsica, the Corsican currents will reintroduce this water into the domain, and one can see how this repeated procedure will ultimately reduce discrepencies between parent and nested models. The root mean square differences between parent and child models is summarized in Tab. 1 for all metrics.

5 Conclusions

When a nested model is available, it usually benefits from higher resolution, and improved representation of some relevant processes. However often, and particularly so in the operational oceanography context, there is no feedback from the nested model to the parent model. Data exchanges are limited to the parent model providing initial and/or boundary conditions to the nested model. Thus, the benefit of having a nested model is lost to the parent model.

Metric	Free model	Upscaled model
Cross-shelf transport [m^3/s]	99.6 10^3	85.2 10^3
N.C. intensity [Sv]	0.22	0.19
Rhône Plume [km]	95.1	88.0
SST [$^\circ$C]	1.3	1.3
WMDW [km^3]	1563	1422

Table 1. Root Mean Square difference between parent and child model for the case of the free parent model and the upscaled parent model, for the defined metrics

The upscaling method consists in assimilating results from a regional model into a basin-wide model, in order to emulate the feedback of two-way nesting. The underlying hypothesis is that the nested model is more realistic than the parent model.

The method was tried out using a nested model configuration of the Mediterranean Sea and the North-Western basin, with a resolution ratio of 5. Data assimilation was performed using a localized ensemble Kalman Transform filter; as pseudo-observations, thinned 3D fields of temperature and salinity were used. The aim of this study is limited to verifying whether nesting feedback could be emulated by data assimilation; without trying to verify whether the nested model is indeed more realistic than the parent one.

Whether upscaling was able to emulate two-way nesting, was measured using 5 metrics related to processes relevant in the study domain: the intensity of the Northern Current, the cross-shelf transport, the position of the Rhône river plume, sea surface temperature, and the quantity of Western Mediterranean Deep Water. These metrics show that the upscaling method is indeed able to emulate two-way nesting and bring the parent model closer to the child model. By assimilating only temperature and salinity, velocity and transport metrics were also improved in the parent model. The ability to constrain the cross-shelf transport by T/S assimilation is also an indication that the data from a high-resolution glider fleet would be beneficial to constrain the model. Finally, concerning the Rhône river plume, upscaling was able to strongly modify the plume direction and length in the parent model. Qualitatively, when real chlorophyll observations were available, the nested and upscaled parent model seemed to be more realistic than the free parent model.

Advantages of using upscaling include the following. Most importantly of course, the parent model takes advantage of improvements in the nested model. In the current study, these improvements may be due to higher resolution, better representation of local processes, and the use of more realistic river discharges. In general, they may also have other causes, such as assimilation of local and/or very high resolution measurements (e.g. HF radar observations), atmospheric fields from a regional weather forecasting model, or other more realistic boundary conditions. Another advantage is that over time, discrepencies between parent and nested model are attenuated. The parent model then provides more consistent boundary conditions to the nested model, and artefacts such as wave reflexion at the boundary may be avoided.

In the operational context, a supplementary advantage may appear. If a user is interested in a particular region not entirely covered by a regional model, it may be difficult for him to merge 2 products (the large-scale model, and the finer model not entirely

parameter	parent model	child model
horizontal resolution	8km	1.6km
vertical resolution	31 levels	31 levels
bathymetry	interpolated from GEBCO	interpolated from GEBCO, smoothed at the commen open-sea boundary
surface module	Nemo MFS bulk formula	Nemo MFS bulk formula
surface forcing data	ECMWF Era Interim	ECMWF Era Interim
nudging (damping)	/	/
advection scheme	TVD	TVD
horizontal diffusion	bilaplacian	bilaplacian
vertical diffusion scheme	TKE	TKE
rivers	6 (climatological discharge)	Rhône (daily measured discharge)

Table A1. Model parameters for the parent and child models

covering the area of interest). By default, the user may then use only the coarser model. If the regional model is upscaled into the large-scale model, this is the only product the user needs to consider.

The most important limitation of the method is that the child model should be more realistic than the parent model. Further-
5   more, the coupling with upscaling is not as strong as with real two-way nesting. Other limitations are linked to data assimilation methods and are not different from the assimilation of real observations: (i) the data assimilation procedure itself uses approx-imations, and this could degrade the analysis; (ii) if the parent and child models are very different, the parent model could be unable to ingest the pseudo-observations. These limitations are investigated in the litterature in the context of assimilation of real observations, and potential solutions include (i) anamorphosis techniques (when a non-linear relation exists between
10   model variables and observations), particle filters (when the error distribution cannot be considered Gaussian), etc; and (ii) carefull specification of the observation error covariance matrix (and more specifically the contribution of the representativity error) to filter out processes of the nested model that cannot be represented in the parent model.

Appendix A: Model configuration

NEMO model parameters for the parent and nested models are given in Table A1.

Competing interests. No competing interests are present.

Acknowledgements. This work has been carried out as part of the Copernicus Marine Environment Monitoring Service (CMEMS) UP-SCALING project. CMEMS is implemented by Mercator Ocean in the framework of a delegation agreement with the European Union. Computational resources have been provided by the supercomputing facilities of the Consortium des Equipements de Calcul Intensif en Federation Wallonie-Bruxelles (CECI) funded by the Fond de la Recherche Scientifique de Belgique (FRS-FNRS).

References

Alberola, C., Millot, C., and Font, J.: On the seasonal and mesoscale variabilites of the Northern Current during the PRIMO-0 experiment in the western Mediterranean Sea, Oceanologica Acta, 18, 1995.

Alvarez, A., Lopez, C., Riera, M., Hernandez-Garcia, E., and Tintore, J.: Forecasting the SST space-time variability of the Alboran sea with genetic algorithms, Geophysical Research Letters, 27, 2000.

Auclair, F., Casitas, S., and Marsaleix, P.: Application of an inverse method to coastal modeling, J. Atmos Oceanic Technol, 17, 1368–1391, 2000.

Auclair, F., Marsaleix, P., and Estournel, C.: The penetration of the Northern Current over the Gulf of Lions (Mediterranean) as a downscaling problem, Oceanologica Acta, 24, 529–544, 2001.

Auclair, F., Marsaleix, P., and De Mey, P.: Space-time structure and dynamics of the forecast error in a coastal circulation model of the Gulf of Lions., Dyn. Atmos. Oceans, 36, 309–346, 2003.

Barth, A. and Vandenbulcke, L.: Ocean Assimilation Kit documentation, Universite de Liege, GHER, http://modb.oce.ulg.ac.be/mediawiki/index.php/Ocean Assimilation Kit, 2017.

Barth, A., Alvera-Azcarate, A., Rixen, M., and Beckers, J.: Two-way nested model of mesoscale circulation features in the Ligurian Sea, Progress In Oceanography, 66, 171–189, 2005.

Barth, A., Alvera-Azcarate, A., Beckers, J.-M., Rixen, M., and Vandenbulcke, L.: Multigrid state vector for data assimilation in a two-way nested model of the Ligurian Sea, Journal of Marine Systems, 2006.

Barth, A., Alvera-Azcarate, A., and Weisberg, R. H.: Assimilation of high-frequency radar currents in a nested model of the West Florida shelf, Journal of Geophysical Research, 113, 2008.

Barth, A., Alvera-Azcarate, A., Beckers, J.-M., Staneva, J., Stanev, E., and Schulz-Stellenfleth, J.: Correcting surface winds by assimilating high-frequency radar surface currents in the German Bight, Ocean Dynamics, 61, 599–610, 2011.

Bishop, C., Etherton, B., and Majumdar, S.: Adaptive sampling with the Ensemble Transform Kalman Filter part I: the theoretical aspects., Monthly Weather Review, 129, 420–436, 2001.

Bosse, A., Testor, P., Mortier, L., Prieur, L., Taillandier, V., d'Ortenzio, F., and Coppola, L.: Spreading of Levantine Intermediate Waters by submesoscale coherent vortices in the northwestern Mediterranean Sea as observed with gliders, Journal of Geophysical Research: Oceans, 120, 1599–1622, 2015.

Debreu, L., Vouland, C., and Blayo, E.: AGRIF: Adaptive grid refinement in Fortran, Computers and Geosciences, 8, 8–13, 2008.

Debreu, L., Marchesiello, P., Penven, P., and Cambon, G.: Two-way nesting in split-explicit ocean models: Algorithms, implementation and validation, Ocean Modelling, 49-50, 1 – 21, https://doi.org/https://doi.org/10.1016/j.ocemod.2012.03.003, 2012.

Dee, D. P., Uppala, S. M., Simmons, A. J., Berrisford, P., Poli, P., Kobayashi, S., Andrae, U., Balmaseda, M. A., Balsamo, G., Bauer, P., Bechtold, P., Beljaars, A. C. M., van de Berg, L., Bidlot, J., Bormann, N., Delsol, C., Dragani, R., Fuentes, M., Geer, A. J., Haimberger, L., Healy, S. B., Hersbach, H., Hólm, E. V., Isaksen, L., Kållberg, P., Köhler, M., Matricardi, M., McNally, A. P., Monge-Sanz, B. M., Morcrette, J.-J., Park, B.-K., Peubey, C., de Rosnay, P., Tavolato, C., Thépaut, J.-N., and Vitart, F.: The ERA-Interim reanalysis: configuration and performance of the data assimilation system, Q.J.R. Meteorol. Soc., 137, 553–597, https://doi.org/10.1002/qj.828, 2011.

Guinehut, S., Larnicol, G., and Le Traon, P.: Design of an array of profiling floats in the North Atlantic from model simulations, Journal of Marine Systems, 35, 2002.

Guinehut, S., Le Traon, P., Larnicol, G., and Philipps, S.: Combining ARGO and remote-sensing data to estimate the ocean three-dimensional temperature fields - A first approach based on simulated observations, Journal of Marine Systems, 46, 85–98, 2004.

Hunt, B., Kostelich, E., and Szunyogh, I.: Efficient data assimilation for spatiotemporal chaos: A local ensemble transform Kalman filter, Physica D: nonlinear phenomena, 230, 112–126, 2007.

5 Le Traon, P.-Y., Antoine, D., Bentamy, A., Bonekamp, H., Breivik, L., Chapron, B., Corlett, G., Dibarboure, G., DiGiacomo, P., Donlon, C., Faugère, Y., Font, J., Girard-Ardhuin, F., Gohin, F., Johannessen, J., Kamachi, M., Lagerloef, G., Lambin, J., Larnicol, G., Le Borgne, P., Leuliette, E., Lindstrom, E., Martin, M., Maturi, E., Miller, L., Mingsen, L., Morrow, R., Reul, N., Rio, M., Roquet, H., R., S., and Wilkin, J.: Use of satellite observations for operational oceanography: recent achievements and future prospects, Journal of Operational Oceanography, 8, 2015.

10 Madec, G.: NEMO ocean engine, Note du Pôle de modélisation, Institut Pierre-Simon Laplace(IPSL), France, No 27, ISSN No 1288-1619, 2008.

Mason, E., Molemaker, J., Shchepetkin, A. F., Colas, F., McWilliams, J. C., and Sangrà, P.: Procedures for offline grid nesting in regional ocean models, Ocean Modelling, 35, 1–15, https://doi.org/10.1016/j.ocemod.2010.05.007, 2010.

Millot, C.: Circulation in the Western Mediterranean Sea, Journal of Marine Systems, 20, 423–442, 1999.

15 Nerger, L., Janjic, T., Schroter, J., and Hiller, W.: A regulated localization scheme for ensemble-based Kalman filters, Q. J. R. Meteorol. Soc, 138, 802–812, 2012.

Onken, R., Robinson, A. R., Kantha, L., Lozano, C. J., Haley, P. J., and Carniel, S.: A rapid response nowcast/forecast system using multiply nested ocean models and distributed data systems, Journal of Marine Systems, 56, 2005.

Pinardi, N., Zavatarelli, M., Adani, M., Coppini, G., Fratianni, C., Oddo, P., Simoncelli, S., Tonani, M., Lyubartsev, V., Dobricic, S., and
20 Bonaduce, A.: Mediterranean Sea large-scale low-frequency ocean variability and water mass formation rates from 1987 to 2007: A retrospective analysis, Progress in Oceanography, 132, 318 – 332, https://doi.org/https://doi.org/10.1016/j.pocean.2013.11.003, http://www.sciencedirect.com/science/article/pii/S007966111300222X, 2015.

Schulz-Stellenfleth, J. and Stanev, E.: Analysis of the upscaling problem - A case study for the barotropic dynamics in the North Sea and the German Bight, Ocean Modelling, 100, 109–124, 2016.

25 Simoncelli, S. and Pinardi, N.: Water mass formation processes in the Mediterranean sea over the past 30 years, Journal of Operational Oceanography, 11, S1–S142, https://doi.org/10.1080/1755876X.2018.1489208, 2018.

Simoncelli, S., Pinardi, N., Oddo, P., Mariano, A., Montanari, G., Rinaldi, A., and Deserti, M.: Coastal Rapid Environmental Assessment in the Northern Adriatic Sea, Dynamics of Atmospheres and Oceans, 52, 250–283, https://doi.org/10.1016/j.dynatmoce.2011.04.004, 2011.

Somot, S., Houpert, L., Sevault, F., Testor, P., Bosse, A., Taupier-Letage, I., Bouin, M.-N., Waldman, R., Cassou, C., Sanchez-Gomez, E.,
30 Durrieu de Madron, X., Adloff, F., Nabat, P., and Herrmann, M.: Characterizing, modelling and understanding the climate variability of the deep water formation in the North-Western Mediterranean Sea, Climate Dynamics, 51, 1179–1210, https://doi.org/10.1007/s00382-016-3295-0, https://doi.org/10.1007/s00382-016-3295-0, 2018.

Tippett, M. K., Anderson, J. L., Bishop, C. H., Hamill, T. M., and Whitaker, J. S.: Ensemble Square Root Filters, Monthly Weather Review, 131, 1485–1490, 2003.

35 Vandenbulcke, L., Beckers, J., and Barth, A.: Correction of inertial oscillations by assimilation of HF radar data in a model of the Ligurian Sea, Ocean Dynamics, 67, 117–135, 2017.

Wang, X., Bishop, C. H., and Julier, S. J.: Which Is Better, an Ensemble of Positive–Negative Pairs or a Centered Spherical Simplex Ensemble?, Monthly Weather Review, 132, 1590–1605, 2004.